Surface magnetism of iron borate

V. E. Zubov, G. S. Krinchik, V. N. Seleznev, and M. B. Strugatskiǐ

I. M. Lomonosov State University, Moscow and M. V. Frunze State University, Simferopol

Using the magnetooptic method, we have observed and investigated surface magnetism—i.e., macroscopic magnetic transition layers caused by the magnetic anisotropy of the surface region—on the natural nonbasal facets of single-crystal iron borate (FeBO$_3$). This anisotropy is a consequence of the altered symmetry of the environment of magnetic ions at the surface. Erasure of this surface magnetism at type ($10\bar{1}4$) surfaces takes place in a field $H_{cr} \approx 1.6$ kOe. We construct a theory which allows us to compute the surface anisotropy energy at the ($10\bar{1}4$) and ($11\bar{2}0$) facets; this theory correctly reflects the symmetry of the magnetic anisotropy, and the calculated value of the field H_{cr} is in order-of-magnitude agreement with the measured fields.

1. INTRODUCTION

Surface magnetism, a phenomenon which is caused by the presence of surface-induced anisotropy, has been observed and investigated on the nonbasal type (100) facets of hematite.[1] The appearance of this surface magnetic anisotropy at the nonbasal facets of α-Fe$_2$O$_3$ is caused by the altered symmetry of the environment of magnetic Fe^{3+} ions at the surface compared to the bulk. The field at which the surface magnetization goes into saturation is ~ 20 kOe. Magnetooptic studies of the rare-earth orthoferrites reveal a strong shift in the spin-reorientation transition temperature at the surface in the high-temperature region, which indicates the existence of surface magnetism in these crystals.[2] The possibility of surface magnetism was pointed out long ago by Néel[3]; however, experimental observation of surface anisotropy was hindered by its relatively small magnitude. Favorable conditions for investigating surface anisotropy are found in weak ferromagnets with the easy-plane type of magnetic anisotropy, in particular a demagnetization field energy which is small compared to the usual ferromagnetic energies because of the smallness of the resulting magnetic moment and the near-absence of magnetic anisotropy in the basal plane. The latter circumstance leads to an increased role for surface anisotropy in the magnetization process for weakly ferromagnetic crystals. These conditions are well satisfied in hematite above the Morin point and in rare-earth orthoferrites near the spin reorientation transition temperature.

In Ref. 4 a study was made of the domain structure in single-crystal iron borate FeBO$_3$, a weak ferromagnet with the easy-plane type of magnetic anisotropy. On natural nonbasal facets of FeBO$_3$ there was observed a labyrinthine domain structure similar to the domain structure of thin-film single-magnetic-domain material. In order for a labyrinthine domain structure to appear it is necessary for a perpendicular magnetic anisotropy to be present. Because symmetry conditions forbid any uniaxial basal-plane anisotropy in bulk FeBO$_3$ crystals, it is natural to assume that there is surface magnetic anisotropy at the nonbasal facets of iron borate.

In this paper we have observed and investigated surface magnetism at the nonbasal facets of FeBO$_3$ using magnetooptic methods, and have calculated the surface anisotropy energy for two types of facets—($10\bar{1}4$) and ($11\bar{2}0$)—assuming that this energy is due to magnetic dipole interactions between Fe^{3+} ions. The theory we have developed correctly reflects the observed symmetry of the surface anisotropy, and the calculated saturation field for the surface magnetization coincides in order of magnitude with the measured fields.

2. MEASUREMENT METHODS AND SAMPLES

The magnetooptic investigation of FeBO$_3$ was carried out by using the equatorial and polar Kerr effects (EKE and PKE). The EKE consists of a change in the light intensity reflected from the ferromagnet as it is magnetized; its value is proportional to the magnetization component lying in the plane of the ferromagnetic reflector which is perpendicular to the plane of the incident light. The PKE consists of rotation of the plane of polarization of reflected light as the crystal is magnetized; its magnitude is proportional to the component of magnetization perpendicular to the reflecting plane. Because the Kerr effect is proportional to the magnetization, while the depth at which the reflected light originates amounts to at most a few tens of fractions of microns,[5] by using magnetooptic effects we can measure the magnetization curves of thin near-surface layers on the sample.

In this study we used a dynamic magnetooptic setup with automatic recording of the signal, analogous to the one described in Ref. 6. Measurements of the volume magnetic properties of the crystal were carried out using a balance setup, which consisted of a solenoid and two measurement coils. The measurement coils are connected opposite one another and are fitted inside the solenoid, through which an AC current flows at a sonic frequency (90 Hz). The signal which appears when the sample is inserted in one of the coils is measured with a resonant amplifier and is recorded using a chart recorder.

The magnetooptic effect was investigated at the natural facets of bulk single-crystal FeBO$_3$. Because application of the usual technology for making single-crystal iron borate, which involves growth from a solution in a melt, usually results in very fine plate-shaped samples whose surfaces are parallel to the basal plane, the crystals used in this paper were made by gas-phase synthesis, a method which yields bulk crystals.[7] The samples had facets of the following types: ($10\bar{1}4$), ($11\bar{2}0$), ($11\bar{2}3$), and (0001).[1)] For this paper, we studied carefully-grown ($10\bar{1}4$) and ($11\bar{2}0$) facets, of which those with areas of 5–20 mm^2 had plane mirror surfaces. The facet type was determined by the method of optical goniometry, and refined with x-ray diffraction. Using x-ray dif-
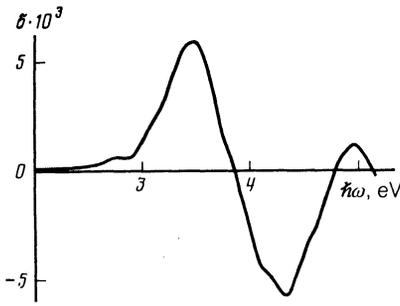
FIG. 1. Spectral dependence of the EKE (δ) at the ($10\bar{1}4$) facet of a $FeBO_3$ crystal. The field **H** is perpendicular to the line of intersection of the ($10\bar{1}4$) and (0001) planes. From here on, the angle of incidence of the light equals $55°$.
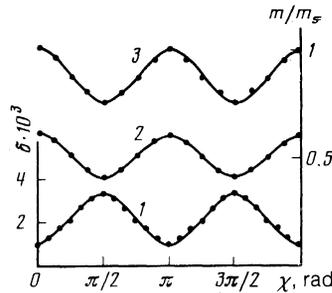

FIG. 2. Curve 1—angular dependence of the EKE ($\hbar\omega = 3.3$ eV, $\varphi = 55°$) at the ($10\bar{1}4$) facet; curves 2,3—angular dependences of the projections of the bulk magnetization onto the direction of **H** as the sample is rotated in the ($10\bar{1}4$) plane, in fields $H = 50$ and 500 Oe, respectively. The angle χ is measured from the line of intersection of the ($10\bar{1}4$) and (0001) planes.

fraction analysis we checked for agreement of the crystal lattice parameters with the data in the literature. The disagreement of the measured parameters with previously published data[8] came to less than 0.01%.

3. EXPERIMENTAL RESULTS

Figure 1 shows the spectral dependence of the EKE measured at a ($10\bar{1}4$) facet of a $FeBO_3$ crystal in the range of photon energies $\hbar\omega = 2$–5 eV. An AC magnetic field with an amplitude of $H = 400$ Oe is applied within the plane of the facet in the [$01\bar{1}0$] direction, which is perpendicular to the line of intersection of the ($10\bar{1}4$) and (0001) facets. The spectral dependence of the EKE at nonbasal facets of bulk crystals of $FeBO_3$ practically coincides with the analogous dependences of the EKE measured in Ref. 9 in the range $\hbar\omega = 2$–3.8 eV on platelike crystals of $FeBO_3$ whose surfaces were parallel to the basal facet. In addition to the peaks observed earlier at $\hbar\omega = 2.8$ and 3.5 eV (Ref. 9), the EKE curve also exhibits features at energies 4.1, 4.3, 4.6, and 5 eV.

In Fig. 2 we show the angular dependence of the EKE (curve 1) taken on the ($10\bar{1}4$) facet at $\hbar\omega = 3.3$ eV in a field $H = 50$ Oe. The angle χ it the plane of the facet is measured from the line of intersection of the planes ($10\bar{1}4$) and (0001). Curve 2 gives the χ dependence of the projection of the magnetization onto the external field direction in the bulk of the sample when it is rotated in the ($10\bar{1}4$) plane; this dependence is measured in the same field ($H = 50$ Oe) as in Fig. 1. Curve 3 was measured in the same way as curve 2, but in a field $H = 500$ Oe; for this field the sample was magnetized to saturation. The projection of the spontaneous magnetization onto the field for $\chi = \pi/2$ equals 0.75 m_s (m_s is the reduced magnetization of $FeBO_3$, see below), which agrees with the calculated value 0.74 m_s since the angle be-

tween the planes (0001) and ($10\bar{1}4$) equals $42°$. There is some discrepancy in the ratios of the magnetization values at the maximum and the minimum for curves 2 and 3, which is apparently due to differences in the projections of the field on the basal plane for the directions $\chi = 0$ and $\chi = \pi/2$ and to difference in demagnetization factors for $\chi = 0$ and $\chi = \pi/2$ because of the irregular shapes of the samples.

It is clear from Fig. 2 that the behavior of the magnetization at the surface differs sharply from that of the bulk magnetization (see, e.g., curves 1 and 2, which were measured at the same field). The variation of the projection of the bulk magnetization onto the field direction as the sample is rotated in the ($10\bar{1}4$) facet plane is related to the fact that the weak ferromagnetic moment in $FeBO_3$, because of symmetry conditions, always lies in the (0001) plane.[7] Therefore, the maximum value for curve 2 is reached for $\chi = 0$, at which angle the field is parallel to the (0001) plane, while its minimum is reached for $\chi = \pi/2$, where the angle between the field and the (0001) plane is maximized. In contrast to the case of bulk magnetization, the maximum value of the EKE for curve 1 occurs at $\chi = \pi/2$ and the minimum at $\chi = 0$. From this we can conclude that a uniaxial magnetic anisotropy is present at the surfaces of ($10\bar{1}4$) facets with easy-axis (EA) magnetization along the [$42\bar{6}\bar{1}$] axis perpendicular to the line of intersection of the ($10\bar{1}4$) and (0001) planes.

Figure 3 shows the field dependence of the EKE for the difficult-axis (DA) and EA magnetization directions (curves 1 and 2, for $\chi = 0$ and $\chi = \pi/2$, respectively). In the surface EA direction the magnetization is practically complete at a field $H \sim 300$ Oe [see Fig. 3(a)], while in the DA direction the EKE reaches a maximum in a field $H \sim 4$ kOe.
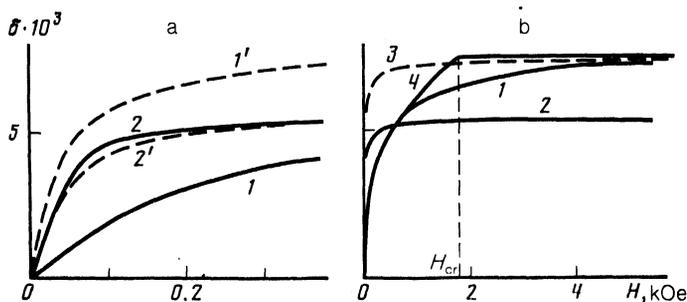

FIG. 3. Field dependence of the EKE ($\hbar\omega = 3.3$ eV) at the ($10\bar{1}4$) facet along the DA (curve 1, $\chi = 0$) and EA (curve 2, $\chi = \pi/2$). The dashed curves in Fig. 3 (a) denote bulk magnetization curves in arbitrary units (curves 1 and 1', 2 and 2' correspond to the same directions of magnetizing field). Curve 3 is a renormalized version of curve 2, as pointed out in the text; curve 4 is the surface magnetization curve at the ($10\bar{1}4$) facet along the DA with a critical field $H_{cr} = 1.6$ kOe, calculated using Eqs. (20) and (21).
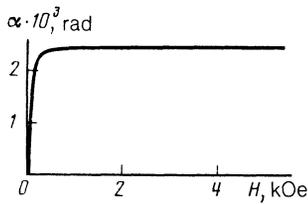
FIG. 4. Field dependence of the PKE (α) at the $(10\bar{1}4)$ facet for $\hbar\omega = 3.3$ eV, which is proportional to the component of the magnetization normal to the facet; $H\perp(10\bar{1}4)$.

As we ought to expect, for $\chi = 0$ the maximum value of the effect exceeds the EKE in the $\chi = \pi/2$ direction.

The magnetization of a FeBO$_3$ crystal is determined by the component of the external field lying in the basal plane, i.e., the plane in which the resulting weak ferromagnetic moment is located. For magnetization along the EA ($\chi = \pi/2$) in the $(10\bar{1}4)$ plane, the projection of the field on the (0001) plane is $H\cos 42° = 0.74\,H$, while for $\chi = 0$ the field is parallel to the basal plane. Curve 3 in Fig. 3(b) was drawn using curve 2, taking into account the projection of the field $\mathbf{H}$ on the basal plane $(0.74\,H)$ and the fact that the maximum value of the EKE along the EA amounts to 74% of the analogous value of the EKE along the DA. In Fig. 3, we use dashed curves to show the bulk magnetization curves in relative units along the $\chi = 0$ (curve 1) and $\chi = \pi/2$ (curve 2) directions in the $(10\bar{1}4)$ plane.

In Fig. 4 we show the field dependence of the PKE for $\hbar\omega = 3.3$ eV for the $(10\bar{1}4)$ facet, which is proportional to the normal component of the magnetization. The spectral dependence of the PKE is close to that of the EKE spectral curve in form (see Fig. 1). Saturation of the PKE takes place in a field ~ 300 Oe, which agrees with the results of measuring the component of magnetization in the $(10\bar{1}4)$ plane (see Fig. 3).

The results presented in Figs. 2–4 allow us to conclude that there exists a surface magnetic anisotropy on the $(10\bar{1}4)$ facet of iron borate, with a critical magnetization field along the DA of $H_{\mathrm{cr}} \approx 1.6$ kOe which was determined from the theoretical curve 4 (Fig. 3) calculated in Sec. 5. In the absence of a field, the magnetization at the facet surface lies in the basal plane along the direction $[2\bar{1}\bar{3}0]$. In this case the magnetization component normal to the facet equals $m_s \sin 42° = 0.67\,m_s$. The slow approach of curve 1 to saturation compared to curve 4 is apparently due to the gradual change of the magnetooptic signal from sinusoidal to rectangular form in fields close to the saturation field. We also seem to observe the persistence effect exhibited by the bulk magneti-

zation curves as measured by the induction method, because the saturation magnetic induction of iron borate at room temperature amounts to 115 gauss (Ref. 10), while the saturation field for the bulk magnetization curves (1′ and 2′ in Fig. 3) amounts to ~ 300 Oe. This effect can also be explained by variation of the magnetic induction signal in the measurement coil when the magnetic field amplitude is close to the saturation field of the magnetization in the bulk.

In Fig. 5 we show the results of investigations of the surface magnetic anisotropy at the $(11\bar{2}0)$ plane, which makes an angle of 90° with the basal plane. Surface magnetization curves are given for two directions: in the plane of the facet parallel to the line of intersection of the (0001) and $(11\bar{2}0)$ planes, i.e., the direction $[\bar{1}100]$ (curve 1), and perpendicular to this line, i.e., the direction $[11\bar{2}0]$ (curve 2). These curves were measured using EKE and PKE, respectively. The dashed curves in the figure denote the bulk magnetization curves in arbitrary units (curves 1′ and 2′), corresponding to the same field directions for which the surface magnetization curves were measured. It is clear from the figure that surface magnetization takes place in the same fields for the two directions; furthermore, there is very little difference between the surface and bulk magnetization curves, i.e., curves 1 and 1′ for magnetization in the plane of the facet and curves 2 and 2′ for magnetization perpendicular to the facet. This implies that there is no detectable surface anisotropy on the $(11\bar{2}0)$ facet, at least to the accuracy that we determine the magnitude of the demagnetization field $(\sim 100$ Oe$)$.

4. THEORY OF SURFACE MAGNETISM

Iron borate—i.e., FeBO$_3$—is a weak ferromagnet with the easy plane type of magnetic anisotropy. The space group of the crystal lattice symmetry is D_{3d}^6. The part of the thermodynamic potential of FeBO$_3$ which is essential to the following discussion has the form[11]:

$$F = {}^1/_2 B\mathbf{m}^2 + {}^1/_2 a l_z^2 + D(l_x m_y - l_y m_x),\qquad(1)$$

where the first term is the exchange energy, the second the uniaxial anisotropy, and the third the Dzyaloshinski energy, which causes the weak ferromagnetism; the l_i ($i = x,y,z$) are the components of the normalized antiferromagnetic vector $\mathbf{l}$ ($\mathbf{l} = (\mathbf{I}_1 - \mathbf{I}_2)/2I$, $I = |\mathbf{I}_1| = |\mathbf{I}_2|$, $\mathbf{I}_1$ and $\mathbf{I}_2$ are the sublattice magnetizations), while the m_i are the components of the normalized ferromagnetic vector $\mathbf{m}$ ($\mathbf{m} = (\mathbf{I}_1 + \mathbf{I}_2)/2I$). From here on, the z axis will coincide with the third-order axis of the crystal, while the x- and y-axes will lie in the basal plane; the x-axis is directed along the second-order axis
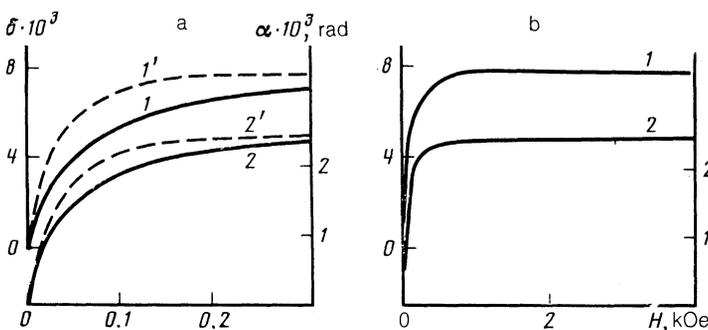

FIG. 5. Field dependence of the EKE (δ) (curve 1) and PKE (α) (curve 2) for $\hbar\omega = 3.3$ eV at the $(11\bar{2}0)$ facet; the facet $(11\bar{2}0)\perp(0001)$. For the EKE, $\mathbf{H}$ is parallel to the line of intersection of the $(11\bar{2}0)$ and (0001) facets; for the PKE, $\mathbf{H}\perp(11\bar{2}0)$. The dashed curves are bulk magnetization curves in relative units (curves 1 and 1′, 2 and 2′ correspond to the same directions of magnetizating field).

while the y-axis lies in the symmetry plane of the crystal. The constant a can be determined once we know the effective uniaxial anisotropy field $H_a = 3$ kOe (at $T = 4$ K), which is measured using antiferromagnetic resonance,[12] and the sublattice magnetization $I = 520$ cgs units ($T = 0$ K; see Ref. 7): $a = 2IH_a = 3.12 \times 10^6$ erg/cm³. The Dzyaloshinski constant is $D = 2IH_D = 1.04 \times 10^8$ erg/cm³, where the Dzyaloshinski field $H_D \approx 100$ kOe at $T = 4$ K.[13] The Dzyaloshinski interaction changes the effective uniaxial anisotropy field[11]; therefore, if we ignore terms which do not depend on the orientation of the vector l, Eq. (1) can be written in the following way:

$$F = (a/2 + D^2/2B)\, l_z^2 = a' l_z^2/2, \qquad (2)$$

where $a' \approx 1.5\, a = 4.68 \times 10^8$ erg/cm³. The constant a' is one of the parameters which determine the structure of the magnetic transition layer from the surface to the bulk crystal (see below).

Equation (2) describes the magnetic anisotropy in a bulk crystal. In the near-surface region the physical picture changes, due to the altered symmetry of the environment of a magnetic ion at the surface compared to the bulk. Let us compute, as in the case of hematite,[1] the contribution of long-range magnetic-dipole interaction to the surface magnetic anisotropy energy. In what follows, we carry out calculations of the surface anisotropy for two types of facets: ($10\bar{1}4$) and ($11\bar{2}0$).

The Case H = 0

The smallest rhombohedron in FeBO₃ with facets of type ($10\bar{1}4$) is illustrated in Fig. 6. The length of this rhombohedron equals 5.9 Å, and the plane angle at the vertex is 104.2°.[7] The surface anisotropy energy at the ($10\bar{1}4$) facet should be invariant under reflection in the yz symmetry plane. Calculations lead to the following form for the surface anisotropy energy at the ($10\bar{1}4$) facet at $T = 0$ K:

$$\sigma_{(10\bar{1}4)}[\text{erg/cm}^2] = -0.043 \sin^2\theta \cos^2\varphi + 0.015 \sin^2\theta \sin^2\varphi$$
$$-0.032 \cos^2\theta + 0.077 \sin\theta \cos\theta \sin\varphi. \qquad (3)$$

This expression is obtained by including the magnetic-dipole interactions of the Fe^{3+} ions located within a rhombohedron similar to the one shown in Fig. 6, with an edge of 20×5.9 Å $= 118$ Å.

In order to calculate the surface anisotropy energy at

FIG. 7. Parallelepiped used to calculate the surface anisotropy energy at the ($11\bar{2}0$) facet of iron borate, which is due to magnetic-dipole interactions among the Fe^{3+} ions. The dimensions of the parallelepiped are 4.6, 8.0, and 14.5 Å along the x, y, and z axes, respectively. The ($11\bar{2}0$) facet is perpendicular to the x axis.

the ($11\bar{2}0$) facet, we used a parallelepiped with dimensions 4.6, 8.0, and 14.5 Å along the x, y, and z axes, respectively, as shown in Fig. 7. The plane $x = $ const is parallel to the ($11\bar{2}0$) facet of the crystal. The surface anisotropy energy at this facet should be invariant relative to rotation around the second-order axes. The calculation gives

$$\sigma_{(11\bar{2}0)}[\text{erg/cm}^2] = -0.008 \sin^2\theta \cos^2\varphi + 0.014 \sin^2\theta \sin^2\varphi$$
$$-0.041 \cos^2\theta - 0.062 \sin\theta \cos\theta \sin\varphi. \qquad (4)$$

Equation (4) is obtained by including the interaction of Fe^{3+} ions located in a parallelepiped with dimensions $92 \times 160 \times 290$ Å. As a control, we calculated the magnetooptic contribution to the effective uniaxial anisotropy field in the bulk crystal; our calculated value was 3.65 kOe, which is in good agreement with the results of Ref. 14, i.e., 3.66 kOe. In this paper we used a special method of summation which speeds the convergence of the dipole sums.

After minimizing Eqs. (3) and (4) with respect to θ and φ, we determine the equilibrium positions of the vector l at the facet surface without including the bulk crystal anisotropy:

$$\theta_0' = 2.64, \quad \varphi_0' = \pi/2 \quad \text{for the } (10\bar{1}4) \text{ facet,}$$
$$\theta_0' = 0.72, \quad \varphi_0' = \pi/2 \quad \text{for the } (11\bar{2}0) \text{ facet.} \qquad (5)$$

Also of interest is the surface anisotropy energy of individual layers of Fe^{3+} ions (σ_i, i is the layer index) located at different distances from the surface. In the table we list the coefficients which appear in the expression for the energy $\sigma_i(\theta,\varphi)$ corresponding to Eq. (3) for the facet ($10\bar{1}4$) at which surface magnetism is observed. It is clear from the table that σ_i decreases rapidly as the layer index increases. Analysis shows that the position of the layer magnetic moment which produces an extremum in $\sigma_i(\theta,\varphi)$ lies in the symmetry plane of the crystal ($\varphi = \pi/2$). In this case σ_i can be written in the following way: $\sigma_i(\varphi = \pi/2) = (\frac{1}{2})a_i \sin^2(\theta - \theta_0^i)$, where θ_0^i is the angle which determines the EA of the ion's magnetic moment in the ith layer. From this we can determine the effective field which acts on the ion's magnetic moment: $H_i = 2a_i/5\mu_B n$, where n is the number of Fe^{3+} ions in a 1 cm² layer area and $5\mu_B$ is the
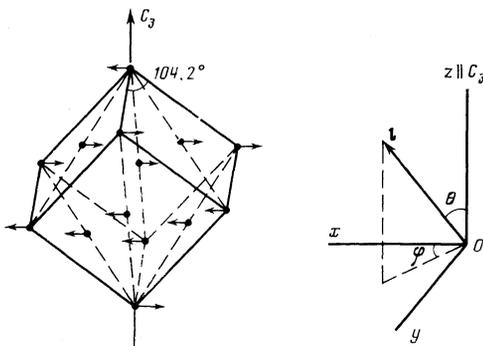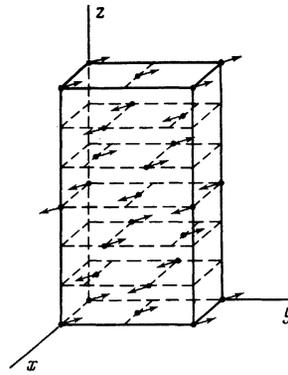

FIG. 6. Smallest rhombohedron in the FeBO₃ crystal with facets of type ($10\bar{1}4$). The length of the rhombohedron edge equals 5.9 Å. At right is shown the coordinate system used.

magnetic moment of a Fe^{3+} ion. The values of a_i, θ_0^i, and H_i are given in the table.

The equilibrium values of the angles θ_0' and φ_0' in (5) at the surface were obtained without including the surface anisotropy of the bulk crystal. When we include this bulk anisotropy, the equilibrium angles θ_0 and φ_0 for the vector l at the facet surface in the absence of an external magnetic field are determined by the competition between the surface anisotropy energy and the energy of the magnetic transition layer; for the case of negligible anisotropy in the basal plane, this competition produces a characteristic variation of the angle θ from its equilibrium value θ_0 at the surface to its equilibrium value in the bulk. The thermodynamic potential of iron borate including the crystallographic magnetic anisotropy energy and the exchange energy connected with inhomogeneity of the vector l can be represented in the form:

$$\Phi = \frac{A_1}{2}\left[\left(\frac{\partial l_\alpha}{\partial x}\right)^2 + \left(\frac{\partial l_\alpha}{\partial y}\right)^2\right] + \frac{A_2}{2}\left(\frac{\partial l_\alpha}{\partial z}\right)^2 + \frac{a'}{2}l_z^2, \quad (6)$$

where $\alpha = x,y,z, A_1, A_2$ are the exchange parameters, and a' is the uniaxial anisotropy constant including the Dzyaloshinski interaction. The energy of the surface transition layer per unit facet area equals:

$$\gamma_\theta = \frac{1}{2}\int_0^\infty\left[A\left(\frac{d\theta}{ds}\right)^2 + a'\cos^2\theta\right]ds, \quad (7)$$

where A is a function of A_1, A_2 and the angle of deviation of the facet measured from the z-axis, s is the distance into the depth of the crystal measured from the surface. The boundary conditions for the problem of calculating the transition layer are:

$$\theta|_{s=0}=\theta_0, \quad \theta|_{s=\infty}=\pi/2, \quad (8)$$

where θ_0 is arbitrary. The form of the function $\theta(s)$ which minimizes the energy γ_θ is determined by solving the corresponding Euler equation. As a result of solving the latter, we obtain in particular

$$\gamma_\theta = \gamma_{\theta_0}(1 - \sin\theta_0), \quad \gamma_{\theta_0} = (a'A)^{1/2}. \quad (9)$$

Let us determine γ_{θ_0}. For $FeBO_3$ the effective exchange field at $T = 0$ K is $H_E = 3\times10^3$ kOe;[15] the exchange constant $B = H_E/I = 5.8\times10^3$ cgs units; $A \approx BI^2c^2$, where $c = 2.7$ Å is the spacing between layers of Fe^{3+} ions. From this we find $A \sim 10^{-6}$ erg/cm^2 and $\gamma_{\theta_0} - 2.2$ erg/cm^2. In these expressions we neglect the anisotropy of the parameter A.

In order to determine the equilibrium magnetic structure of the transition layer near the facet of the crystal, we must find the minimum of the sum of the surface anisotropy energies $\sigma_{(10\bar{1}4)}$ or $\sigma_{(11\bar{2}0)}$ and the transition layer energy γ_θ as a function of the values of the parameters θ_0 and φ_0. The solution of the equations $\partial(\sigma + \gamma_\theta)/\partial\theta_0 = 0$ and $\partial\sigma/\partial\varphi_0 = 0$ lead to the following equilibrium values of the angles:

$$\theta_0 = \pi/2, \quad \varphi_0 = 0 \quad \text{for the } (10\bar{1}4) \text{ facet}, \quad (10)$$

$$\theta_0 = \pi/2, \quad \varphi_0 = 0 \quad \text{for the } (11\bar{2}0) \text{ facet}. \quad (11)$$

It is interesting to note that when the bulk anisotropy is included the equilibrium value of the angle φ_0 [see Eqs. (10), (11)] at the facet surface changes to $\pi/2$, which should be compared to the case (5) (i.e., without including the bulk

anisotropy). In this case the angle θ changes so that the magnetic moments of the Fe^{3+} ions are now located in the basal plane.

The Case $H \neq 0$

Let us now investigate the behavior of the magnetic transition layer in an external field. For the case of relatively small fields ($H \ll H_D$) the thermodynamic potential for a $FeBO_3$ crystal in a magnetic field as a function of the angle φ can be written in the following form:

$$\Phi = (H_D H_t/B)\sin(\psi - \varphi), \quad (12)$$

where H_t is the projection of the field H on the basal plane of the crystal, and ψ is the angle between the direction of H_t and the x-axis. The energy of the transition layer in an external field can be written in the following form:

$$\gamma_\varphi = \int_0^\infty\left[\frac{A}{2}\left(\frac{d\varphi}{ds}\right)^2 + \frac{H_D H_t}{B}\sin(\psi - \varphi)\right]ds. \quad (13)$$

The Euler equation has the form

$$\frac{d\varphi}{ds} = \pm\frac{\sin x}{\delta_{\varphi_0}}, \quad (14)$$

where

$$\delta_{\varphi_0}[\text{cm}] = \frac{1}{2}\left(\frac{AB}{H_D H_t}\right)^{1/2} = \frac{1.2\cdot10^{-4}}{H_t^{1/2}}, \quad x = \frac{\pi}{4} + \frac{\psi}{2} - \frac{\varphi}{2}.$$

The boundary conditions are

$$x|_{s=0} = x_0 = \frac{\pi}{4} + \frac{\psi}{2} - \frac{\varphi_0}{2},$$

$$x|_{s=\infty} = \frac{\pi}{4} + \frac{\psi}{2} - \frac{\varphi + \pi/2}{2} = 0.$$

As a result of substituting (14) into (13), we obtain

$$\gamma_\varphi = \frac{A}{\delta_{\varphi_0}^2}\int_0^\infty\sin^2 x\,ds, \quad ds = \frac{\delta_{\varphi_0}d\varphi}{\sin x}.$$

After an integration we obtain

$$\gamma_\varphi = 2\gamma_{\varphi_0}(1 - \cos x_0), \quad (15)$$

where

$$\gamma_{\varphi_0}[\text{erg/cm}^2] = A/\delta_{\varphi_0} = 0.83\cdot10^{-2}H_t^{1/2}.$$

The surface anisotropy energy of the facets under discussion have the following form for $\theta = \pi/2$:

$$\sigma = b\cos^2\varphi_0 + d\sin^2\varphi_0 = b + (d - b)\sin^2\varphi_0. \quad (16)$$

The angle φ_0 is determined from the equation

$$\partial(\gamma_\varphi + \sigma)/\partial\varphi_0 = -\gamma_{\varphi_0}\sin x_0 + (d - b)\sin 2\varphi_0 = 0. \quad (17)$$

The angle $\varphi = \pi/2$ determines the DA direction for the vector l for both types of facets studied here (for the vector **m**, the direction of the DA coincides with the x-axis). For magnetization along the DA ($\psi = 0$), we obtain from (17)

$$-0.83\cdot10^{-2}H_t^{1/2}\sin(\pi/4 - \varphi_0/2) + (d - b)\sin 2\varphi_0 = 0. \quad (18)$$

For the critical field that disrupts the layer, we obtain from Eq. (18) as $\varphi_0 \to \pi/2$

TABLE I.

Layer index from surface	Coefficient (erg/cm²) of f_j				a_i, erg/cm²	H_i, kOe	θ_0^i, rad
	$f_1 = \sin^2\theta\cos^2\varphi$	$f_2 = \sin^2\theta\sin^2\varphi$	$f_3 = \cos^2\theta$	$f_4 = \sin\theta\cos\theta\sin\varphi$			
1	−0.044	0.020	−0.039	0,083	0,2	14.5	2.67
2	0.06·10⁻²	−0.060·10⁻¹	0,077·10⁻¹	−0.061·10⁻¹	0,03	2.2	1.36
3	0.079·10⁻⁴	0.069·10⁻²	−0.068·10⁻²	−0.018·10⁻²	0.003	0.2	0.07
4	0.08·10⁻⁵	−0.055·10⁻³	0.046·10⁻³	0.084·10⁻³	0.0002	0,02	1,92

$$H_{cr} = 2,3 \cdot 10^5 (d-b)^2. \tag{19}$$

At $T = 0$ K, we have $d - b = 0.058$ erg/cm² [see (3)] and $H_{cr} = 800$ Oe for the $(10\bar{1}4)$ facet, while for the $(11\bar{2}0)$ facet we have $d - b = 0.022$ erg/cm² [see (3)] and $H_{cr} = 110$ Oe. The latter field is comparable in magnitude to demagnetization fields in bulk $FeBO_3$ crystals; therefore it is difficult to observe a surface anisotropy with such a critical field. Let us determine H_{cr} for the $(10\bar{1}4)$ plane at room temperature $(T = 300$ K). Because $A \propto I^2$, $H_D \propto I$, $d - b \propto I^2$, while $I(0)/I(T) = 1.47$ (Ref. 10), we obtain in place of (18) and (19)

$$-0.47 \cdot 10^{-2} H_t^{1/2} \sin(\pi/4 - \varphi_0/2) + (d' - b')\sin 2\varphi_0 = 0, \tag{20}$$

$$H_{cr} = 7.2 \cdot 10^5 (d' - b')^2, \tag{21}$$

where

$$d' - b' = 0.058/(1.47)^2 = 0.027 \text{ erg/cm}^2.$$

From this we obtain H_{cr} $(T = 300$ K$) \approx 500$ Oe. For the $(11\bar{2}0)$ facet this field satisfies H_{cr} $(T = 300$ K$) \approx 70$ Oe at room temperature. Let us estimate the effective width of the transition layer, which is defined as follows:

$$\delta_\varphi \, [\mu m] = \frac{ds}{d\varphi}\bigg|_{\varphi=\varphi_0} \left(\frac{\pi}{2} - \varphi_0\right) = \frac{\delta_{\varphi_0}(\pi/2 - \varphi_0)}{\sin\left(\frac{\pi}{4} - \frac{\varphi_0}{2}\right)} \approx 2\delta_{\varphi_0} = \frac{2}{H_t^{1/2}}.$$

For $H = 100$ Oe $\delta_\varphi = 0.2$ μm at room temperature.

5. DISCUSSION OF EXPERIMENTAL RESULTS

When the values of $d' - b'$ are known, Eq. (20) determines the dependence of the orientation of l at the surface on H_t when the crystal is magnetized along its DA. For a certain critical field H_{cr} the magnetization of the surface layer is driven into saturation, in which case $\varphi_0(H_{cr}) = \pi/2$. The function $\varphi_0(H)$ can also be used to solve the inverse problem, i.e., determining the value of H_{cr} on the basis of a known experimental magnetization curve.

(10̄14) facet. The calculated magnetization curve for the surface layer with $H_{cr} = 1.6$ kOe (curve 4 on the same figure) agrees well with the experimental curve (curve 1 on the same figure) for the $(10\bar{1}4)$ facet in its initial and intermediate regions. The disagreement between the theoretical and experimental curves for $H \sim H_{cr}$ was discussed above (see Sec. 3). The value of H_{cr} for the $(10\bar{1}4)$ calculated using Eq. (21), including the magnetic dipole surface anisotropy energy, comes to ~ 500 Oe, i.e., three times smaller than the experimental value. The DA and EA magnetization directions coincide for theory and experiment. Hence, including the surface anisotropy due to magnetic dipole interac-

tions of the Fe^{3+} ions leads to a qualitative explanation of the observed physical picture, and gives the correct order of magnitude for the field H_{cr}.

(11̄20) facet. On the basis of our investigations of the magnetization curves for surfaces of $(11\bar{2}0)$ type facets given in Fig. 5, we can conclude that to the accuracy determined by the values of the demagnetization fields $(\sim 100$ Oe), surface anisotropy is absent at three facets. This agrees with the calculated value of the field $H_{cr} \approx 70$ Oe.

The disagreement between the theoretical and experimental values of the field H_{cr} for the $(10\bar{1}4)$ facet may be due to a partial surface reconstruction, i.e., to a shift in the Fe^{3+} ions at the surface from positions which they should occupy corresponding to the bulk crystal structure. Such a reconstruction should lead to a considerable change in the magnetic-dipole energy of the Fe^{3+} ions at the surface and near it, because the contribution per unit area of the outer layers of ions to the surface anisotropy is higher than the contribution from the deeper layers. This circumstance is well illustrated in Table I. In addition, the surface anisotropy energy may contain contributions from single-ion anisotropy and the Dzyaloshinski interaction of magnetic ions in the near-surface layer.

In conclusion, we can say that we have added iron borate to the list of weak ferromagnets in which surface magnetism has been observed, a list which previously contained only hematite and the rare-earth orthoferrites. The origin of surface magnetism in these crystals is the change in symmetry of the environment of magnetic ions at the surface. The significant, and in the case of hematite and iron borate, apparently decisive, contribution to the anisotropy energy comes from magnetic-dipole interactions of the magnetic ions.

¹⁾The facet indices refer to a hexagonal coordinate system (see Ref. 7).

¹G. S. Krinchik and V. E. Zubov, Zh. Eksp. Teor. Fiz. **69**, 707 (1975) [Sov. Phys. JETP **42**, 359 (1975)].

²E. A. Balykina, E. A. Gan'shina, and G. S. Krinchik, Zh. Eksp. Teor. Fiz. **93**, 1879 (1987) [Sov. Phys. JETP **66**, 1073 (1987)].

³L. Néel, J. Phys. Radium **15**, 225 (1954).

⁴A. R. Prokopov, V. N. Seleznev, M. B. Strugatskii, and S. V. Yagipov, Zh. Tekh. Fiz. **57**, 2051 (1987) [Sov. Phys. Tech. Phys. **32**, 1241 (1987)].

⁵G. S. Krinchik, V. E. Zubov, and V. A. Lyskov, Opt. Spektrosk. **55**, 204 (1983) [Opt. Spectrosc. (USSR) **55**, 120 (1983)].

⁶G. S. Krinchik and V. E. Zubov, Zh. Eksp. Teor. Fiz. **80**, 229 (1981) [Sov. Phys. JETP **53**, 115 (1981)].

⁷R. Diehl, W. Jantz, B. I. Nölang, and W. Wettling, Curr. Top. Mater. Sci. **11** (Amsterdam: Elsevier Sci. Publ., 1984), pp. 241–387.

⁸R. Diehl, Solid State Commun. **17**, 743 (1975).

⁹I. S. Edel'man and A. V. Makarovskii, Opt. Spektrosk. **35**, 959 (1973) [Opt. Spectrosc. (USSR) **35**, 554 (1973)].

¹⁰A. M. Kadomtseva, R. Z. Levitin, Yu. F. Ionov *et al.*, Fiz. Tverd. Tela (Leningrad) **14**, 214 (1972) [Sov. Phys. Solid State **14**, 172 (1972)].

2127   Sov. Phys. JETP **67** (10), October 1988

Zubov *et al.*   2127

[11]I. E. Dzyaloshinski, Zh. Eksp. Teor. Fiz. **32**, 1547 (1958) [Sov. Phys. JETP **5**, 1259 (1958).

[12]L. V. Velikov, A. S. Prokhorov, E. G. Rubashevskii, and V. N. Seleznev, Pis'ma Zh. Eksp. Teor. Fiz. **15**, 722 (1972) [JETP Lett. **15**, 511 (1972)].

[13]L. V. Velikov, A. S. Prokhorov, E. G. Rubashevskii, and V. N. Seleznev, Zh. Eksp. Teor. Fiz. **66**, 1857 (1974) [Sov. Phys. JETP **39**, 909 (1974)].

[14]V. V. Rubenko, V. N. Seleznev, and A. S. Khlystov, Abstracts from the All-Union Conf. on the Physics of Magnetic Phenomena (Donetsk: Izd. Donetsk. Fiz.-Tekh. In-Ta AN SSSR, 1977), p. 80.

[15]M. Eibschütz and M. E. Lines, Phys. Rev. **B11**, 4907 (1973).

Translated by Frank J. Crowne